Applied Mathematics & Information Sciences
An International Journal

http://dx.doi.org/10.18576/amis/180617

Reliability Risk-Based Analysis and Mitigation Measures of Existing Concrete Gravity Dam

Zakaria Che Muda[1,], Mohamed Hafez[1], Lariyah Mohd Sidek[2], Salmia Beddu[2], Payam Shafigh[3], Zaher Almkahar[1], and As'ad Zakaria[4]*

[1]Faculty of Engineering and Quantity Surveying, INTI-International University, Nilai, Malaysia
[2]Institute of Energy Infrastructure, Nasional Energy University, Selangor, Malaysia
[3]College of Architecture and Energy Engineering, Wenzhou University of Technology, China
[4]Institute of Energy Systems, School of Engineering, University of Edinburgh, Edinburgh, UK

Received: 15 May 2024, Revised: 1 Jul. 2024, Accepted: 10 Jul. 2024.
Published online: 1 Nov. 2024.

Abstract: The paper investigates the suitability of using FORM and Monte Carlo reliability risk analysis for mitigation measures of the existing concrete gravity dam. Many aging gravity dams need rehabilitation resulting from dam safety assessment based on the current stringent safety standards due to climate change. The sliding failure mode is the dominant mode failure over the overturning where its mitigation measures are required for remedial works of the existing dam. Sensitivity analysis of friction angle has the highest sensitivity of 91.2% compared with 8.6% for the density of concrete and cohesion with only 0.2%. The mitigation measure using post-tensioned anchors and raked micro-piles for the probability of sliding failure mode was investigated using the Monte Carlo simulation. There is only a marginal increase in post-tensioning design force and no changes to the micro-pile if the probability of failure needs to be decreased from 10^{-4} to no likelihood of failure under each event scenario. It is prudent to look into these measures as there is no implication on the construction cost and the time for completion. Raked micro-piles provide a better remedial option than post-tensioned anchors as they do not intrude into the main body of the structure nor interrupt the operation of the hydropower plant. Reliability risk analysis using Monte Carlo simulation is a powerful tool that can be utilized in the assessment and mitigation measures of the existing dam.

Keywords: climate change; reliability risk assessment; first-order and Monte Carlo risk analysis; mitigation measures; probability of failure.

1 Introduction

Massive concrete gravity dams have a triangular cross-section designed to maintain stability against external forces by having enough mass and a sufficient base to resist sliding and overturning against external destabilizing forces. The upstream face of the dam is slightly sloped for the component of the water force to push downward to enhance the stability of the structure. A gravity dam consists of a continuous or a series of concrete monoliths separated by expansion joints. Hydroelectric power schemes often used concrete gravity dams in their projects.

Many old gravity dams need rehabilitation resulting from dam safety assessment based on stringent safety standards based on new criteria relating to Probable Maximum Flood (PMF) and Maximum Credible Earthquake (MCE). Concrete gravity dams are more tolerant to earthquake shaking and not subjected to overtopping and piping issues as the embankment or rockfill dams.

Flood, earthquake, and uplift loads are generally larger today due to the extreme climatic risk and abnormal events than assumed in the previous design of most gravity dams while the required factors of safety remain unchanged. Consideration of climate change impacts in dam design and operation is becoming crucial. Incorporating risk-informed decision-making, flexible operational strategies, sediment management plans, and structural design measures can enhance the resilience of dams to changing climate conditions. The influence of climate change in the form of extreme rainfall events plays a substantial role in impacting the Reliability and safety of dams. This highlights its significance and importance in the analysis of dam-related risks.

On the other hand, the efficiency in the operation of hydroelectric power dams is also influenced by the capacity to forecast droughts. Currently, a challenge in many major river basins across Malaysia is the scarcity of quantifiable data about drought incidences and reliable forecasting techniques. The research by Khan et al (2020) concluded that the use of paired models involving Wavelet Analysis-Autoregressive Integrated Moving Average with artificial neural networks represents a reliable approach for the short-term prediction of droughts in Malaysia. Fluixá-Sanmartín

*Corresponding author e-mail: zakaria.chemuda@newinti.edu.my

et. al. (2018) presents an interdisciplinary review of the state-of-the-art research on projected climate change impacts on dam safety attending to both climatic and non-climatic drivers. The structure followed for such a review is based on the risk analysis approach in which all the variables concerning dam safety – from the hydrological loads to the consequences of failure – and their interdependencies are included comprehensively.

As a result, many existing dams have marginal or unsatisfactory calculated stability using modern guidelines. To meet the modern design standards to comply with the probable maximum flood and maximum credible earthquake demand or extension of the life program, many dams need to be rehabilitated and strengthened. Further raising operation needs, ageing, deterioration deficiencies in design and construction of an old concrete dam in the first half of century where owners are obliged by statutory regulations to take remedial action.

Gravity dam primary failure modes are mainly caused by the instability of the dam-foundation interface and its failure mechanism is dependent on it (Su et al, 2013). It is necessary to assess the reliability risk analysis under different failure modes and its instability probability of failure could be ranked accordingly against the ICOLD (2005) probability failure criterion and USBR-USACE (2019) Dam Risk Matrix.

The majority of failure cases in concrete dams involved foundation problems. ICOLD (1995) gives a summary of the reasons for concrete dam failure cases as follows;

1 Foundation problems such as shear strength, seepage, and internal erosion - 48 % of case failures.

2 Actions of exceptional magnitude - 24 % of the case failures

3 Due to concrete such as tensile stresses and ageing - 14 % of case failures

4 Due to structural behavior - 14 % of the failure cases.

Xu and Benmokrane (1996) reviewed the strengthening of existing dams using post-tensioned anchors and listed the main reasons for mitigation as follows;

1 stringent changes in safety standards

2 deficiencies in design and construction

3 loss of strength due to concrete ageing and deterioration

4 increase the height of the dam

In the early fall of 2005, the Gilboa Dam had a service performance issue in that the sliding stability of the spillway structure did not meet the New York State dam safety criteria and was strengthened using high-capacity rock anchors (Zicko et al., 2007). Post-tensioned anchors are the most viable and cost-effective solution for strengthening existing concrete dams. The ground anchors are the provision of resistance against uplift, sliding, overturning, and seismic loadings. The post-tensioning technique required minimum demolition without reconfiguring the existing dam and did not interrupt its running operation.

Fig. 1 illustrates the use of post-tensioned rock anchors in stabilizing concrete gravity dams against (a) overturning and (b) downstream sliding with the forces involved in a limiting equilibrium analysis.

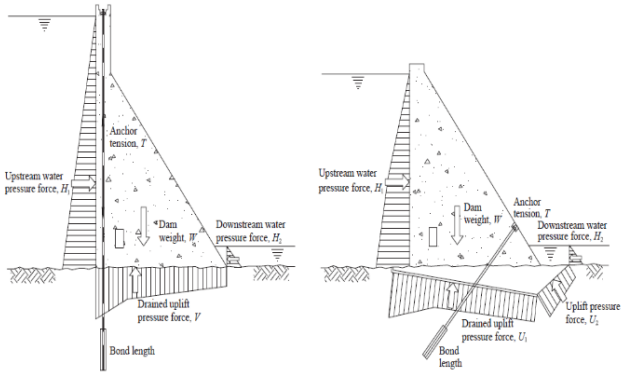

(a) (b)

Fig. 1: Post-tensioned anchors to resist (a) overturning and (b) downstream sliding

(Adapted from ANCOLD, 1992; USACE, 1995)

The conventional design of concrete gravity dams still follows the deterministic method, which does not directly account for the effect of uncertainties of the input variables on the safety of structures (Pires et al., 2019). The usual engineering design code of practice still uses the normal deterministic approach with the given safety factor to determine the elemental or overall stability of structures. Safety factors have been based on a deterministic approach based on the mean values of the data obtained regardless of the variance of the data that has been widely incorporated in the design criteria worldwide. The argument is that the project meeting the higher safety factors would be sufficiently safe than the one with the lower safety factor; unfortunately, this is not always true. The wide variance of the data with a higher safety factor is not the same as a narrow variance of the data with a lower safety factor. A given safety factor with a higher variance returns a higher probability of failure than the one with a narrow variance depending on the uncertainties in the input data, such as coefficient of variation, number of tests, quality of investigations, measurement techniques, etc. Thus, the structural safety achieved through these safety factors can vary over a wide range of values in terms of its probability of failure (ICOLD, 1993).

The traditional safety factors approach often lacks the real picture in assessing the actual safety of dams. Dams designed with similar safety factors may give various probabilities of failure. A probabilistic analysis is considered a more appropriate method to enhance the true Reliability of a dam's

structural safety.

The probabilistic analysis calculations offer a visible and all-embracing representation of the affecting variables in dam safety. This analytical method reveals the influencing factors are most sensitive and exert a significant effect on the probability of dam failure. Hariri-Ardebili (2018) provides a comprehensive state-of-the-art review of an effective risk-based approach that is tied to the probabilistic method for dam safety covering the fundamental elements in uncertainty quantification, terminologies, and their interconnections. Pires et al. (2019) conducted a practical demonstration of the use of structural reliability theory in the case study of a constructed concrete gravity dam.

Their study identified the critical failure modes and design variables that produced the most significant impact on the dam's safety. The practical application of structural reliability techniques is not yet widely prevalent in the field of concrete dams (Pires et al., 2019). Reliability analysis is intricately related to the computation and prognosis of the probability of failure of a structural system at any point of time in its operational lifecycle (Melchers and Beck 2018). The probability of failure is governed through the use of structural reliability analysis.

Structural reliability analysis utilizes probabilistic approaches to evaluate the safety of a given structure (Garcia et al., 2012). Christian et al. (1994) and Tang et al. (1999), provide clear underlying theories and examples of the use of Reliability in geotechnical engineering. The conventional factor of safety approach to limit state problems provides very limited insight into the failure probability of the structural system. Reliability calculations act as a valuable means for measuring the cumulative influence of uncertainties and for distinguishing between scenarios of varying degrees of uncertainty, particularly high or low.

This reliability analysis sometimes mentioned as the probability of failure should not be viewed as a replacement for the traditional deterministic approach using the factor of safety but rather as a supplement to each other that will add value to the analysis (Duncan, 2000). Incorporating reliability analysis into the design and safety assessment of concrete gravity dams provides a rational method to address the limitations innate in the traditional safety factor approach (Pei et al, 2011, Sharafati et al., 2020). The use of safety factors for safety quantification of structures should be used with limitations and caution as the structure with the same safety factors but different coefficients of variation can result in the variation in probabilities of failure in the order 10^{-4} (ICOLD, 1993).

The reliability analyses provide more reliable results and a more logical framework than the factors of safety when the relationship between the probability of failure, and its consequences of failure in terms of life and economics need to be established with a higher degree of accuracy. Probabilistic analyses offer a more *comprehensive* and inclusive *assessment* compared to deterministic analyses in which the inherent variability in input variables is taken into consideration into the likelihood of failures. This approach demands a more extensive dataset in terms of expected variations and the probable probability distributions of these variables (Muench, 2010).

First Order Reliability Method (FORM) can be applied to stability analysis of the dam block through simple procedures and need not require more data than is required for conventional analyses using the factor of safety. A relatively small additional effort can significantly increase the added value obtained from these analyses (Yang and Ching, 2020). Monte Carlo Simulation (MCS) requires a large number of calculations to obtain the results with high accuracy, where the computational cost is relatively large. Monte Carlo Simulation (MCS) requires a large number of calculations to obtain the results with high accuracy, where the computational cost is relatively large.

Risk is defined as the product of the probability of a critical event, a system of failure of the given event, and its consequences according to Equation (1).

$$Risk = \sum P(Critical\ event) \times \sum P(System\ of\ failure\ of\ the\ event) \times C\ (consequences) \quad (1)$$

The risk related to dam failure measures the likelihood or probability of the consequences on life and the cost of damage to the property and the environment.

The International Commission on Large Dams (ICOLD) stated that the application of risk analysis serves as an important instrument in the risk management process. The process of dam risk analysis involves identifying potential failure modes and quantifying the structural system responses to various loading conditions (ICOLD, 2005).

During the construction and operation stage, the use of instrumented measured uplift and shear strength with thorough knowledge of site geology will reduce the uncertainty in stability evaluations of the risk analysis and economic cost.

The objective of this paper is to assess the suitability of using the FORM-Taylor series analysis and Monte Carlo simulation for risk-based assessment and mitigation measures of the existing concrete gravity dam that did not comply with the ICOLD (2005) and USBR-USACE (2019) guidelines.

2 Tolerable risk guidelines

A risk matrix serves as a useful tool for visually representing the likelihood of failure against the potential consequences linked to the known risk drivers of significance in nature. Fig. 1 illustrates a risk matrix employing general categories for the likelihood of failure and consequence category with economic and life loss. The vertical axis is the likelihood of failure and the annual probability of failure, while the horizontal axis denotes the associated outcomes of loss of life and economic implications (USBR-USACE, 2019).

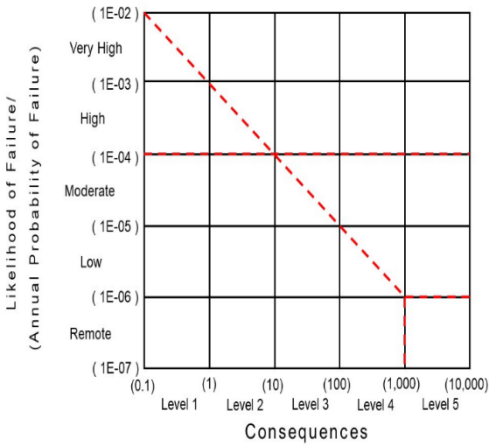

Fig. 2: Dam Risk Matrix: adopted from USBR-USACE (2019)

However, further studies need to be carried out on the life and economic loss as a consequence of the probability of failure associated with the dams. ICOLD (2005) uses the horizontal dashed line value for the probability of failure of 10^{-4} for high-risk dams.

For existing dams, based on ANCOLD (2003) Individual Life Safety Risk Guideline criterion that should be less than a limit value of 1 in 10,000 per year, except in exceptional circumstances and societal risk guidelines for existing dams where the annual probability of failure against the loss of life varies from 1E-3 to 1E-6 or less for 1 and 1000 loss of life respectively.

The U.S. Army Corps of Engineers (USACE, 2014) policy stated concerning the estimated annual probability of failure (APF) as follows:

1 APF > 1 in 10,000 per year: When the APF exceeds 1 in 10,000 per year, it is considered unacceptable, with exceptions allowed only under extraordinary circumstances. Reclamation (2003) suggests that the justification for implementing risk reduction measures, if APF estimates, surpass the 0.0001 per year threshold.

2 APF < 1 in 10,000 per year: When the APF is less than 1 in 10,000 per year, it is deemed tolerable if all the other tolerable risk guidelines are fulfilled. Reclamation (2003) stated that as the APF estimates decrease below this mark, the rationale for implementing risk reduction measures diminishes.

3 Reliability-based design methods

The reliability-based analysis of a typical cross-section of the gravity concrete dam is analyzed by First Order Reliability Method (FORM) using first-order Taylor series approximation and compared with a more complex Monte Carlo Simulation (MCS) approach. FORM-Taylor Series approximation is mathematically simpler, though somewhat less precise, that can be performed using an excel spreadsheet that is used by the design practitioners. MCS which is coded in MATLAB provides a more rigorous and precise analysis that is suitable for construction and remedial assessment and a research-based environment.

3.1 First-Order Reliability Method (FORM)

The First-Order Reliability Method (FORM) comes from its fundamental principle, where the performance function g(X) is estimated through the use of a first-order Taylor expansion, thus denoting a linearized approximation.

A performance function or limit state function, $g(x)$ is defined as the failure state ($g(x) < 0$) and safety state ($g(x) > 0$) where $x = (x_1, x_2,..., x_n)$ is a random variable vector.

The performance function (Phoon, 2019) is widely adopted:

$$g\,(x) = g\,(x_1, x_2,..., x_n) = F_s\,(x_1, x_2,..., x_n) - 1.0 \quad (2)$$

Where F_s is the factor of safety and the prescribed acceptable safety factor is 1.0 (Liang et al., 1999).

The probability of failure can be defined as

$$P_f = P\,(g\,(x) < 0) = \int g(x) \leq 0\, f(x)\, dx \quad (3)$$

Where $f(x)$ is the joint probability density function of x.

Because the multidimensional integral in (2) can be very difficult, the reliability index β is generally calculated in engineering, and the failure probability is estimated by

$$P_f \approx \emptyset\,(-\beta) = 1 - \emptyset\,(\beta) \quad (4)$$

$$\text{or } \beta) \approx -\,\emptyset^{-1}\, P_f, \text{ with } \emptyset\,(Z) = \frac{1}{\sqrt{2\pi}} \int_{-\infty}^{Z} e^{-z^2/2}\, dz \quad (5)$$

Where Φ (Z) is the standard normal cumulative distribution function.

Since FORM only gives a linear approximation of the limit-state function at the design point, the reliability index may be over- or underestimated for the functions with considerable curvature.

3.2 Monte Carlo Simulation

Monte Carlo simulation (MCS) allows solving any level of difficulty with a multi-number of the variable of a large complex model with linear or non-linear single or multiple limit state functions. Samples trials of random variables are obtained from the joint density function f(x) in Equation 2. The probability of failure is estimated as in Equation 4.

$$P_{fMCS} = \frac{1}{N} \sum_{i=1}^{N} I[X_i] = \frac{N_f}{N} \quad (6)$$

where P_{fMCS} is the estimated probability of failure, I [ ] is the indicator function, X_i is the sample vector i, N_f is the number of points in the failure domains, and N is the number of trials. The number of trials must be large enough to obtain the accurate probability of failure with the least statistical error.

$$I(X_i) = \left.\begin{array}{l} \\ \end{array}\right\} \; 1 \text{ if } g(x) \leq 0$$

$$0 \text{ if } g(x) > 0$$

Finally, the MCS-based reliability index is given as:

$$\beta_{MCS} \approx - \Phi^{-1} (P_{fMCS}) = \Phi^{-1} (1- Pf_{MCS}) \quad (7)$$

4 Concrete gravity concrete dam – A case study

The concrete dam has a maximum height of about 40 m, a full supply level (FSL) is at 38.00 m EL and design flood level (DFL) is at 40.00 m EL. The overtopping level (OL) is assumed to be 1 m above the crest level at 41.00 m EL. The tailwater level at FSL, DFL and OL is 5.00 m EL. The sedimentation Level is assumed to be 13.30 m EL. The embankment crest is at EL 40.00m with an upstream and downstream embankment slope varying 5(V):1(H) and 1.677(V):1(H) respectively.

Fig. 3 indicates the typical cross-section through the main section of the existing dam under this case study.

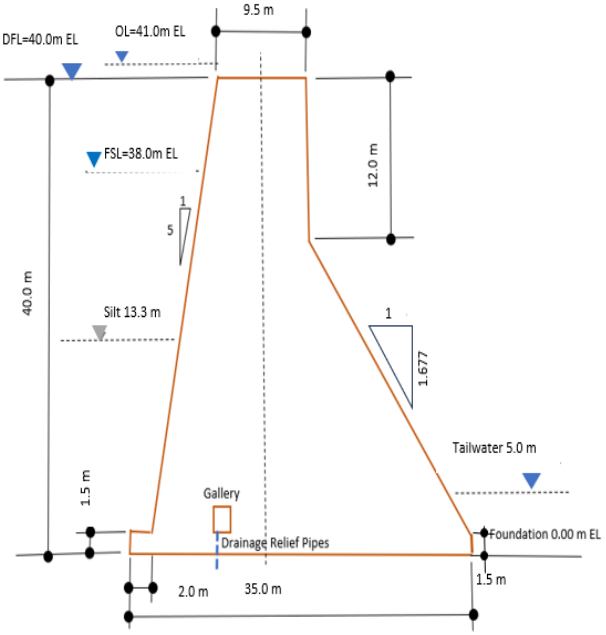

Fig. 3: Typical cross-section through of the main section of the Existing Dam

4.1 Variability of Design Parameters

Variable material parameters involved in the reliability risk analysis of the concrete gravity dam include the density of concrete, shearing friction coefficient and cohesion of dam concrete-rock interface. Volume weight of concrete, friction angle and cohesion were determined by site-specific laboratory test samples. The sample size must meet the statistical requirements and be treated as a random variable (Xin and Chongshi, 2016).

Economic and safety reasons made it desirable to use the actual site-specific values of shear strength and uplift based on the actual monitoring system rather than generic values as specified in the guidelines for concrete dam stability analyses. The use of instrumented measured uplift and shear strength with thorough knowledge of site geology will reduce the uncertainty in stability evaluations of the risk analysis and economic cost. Uplift pressures over the maximum design have been reported in some dams (Spross, J. et al., 2014). Degradation phenomena in dam-foundation contacts have been also reported in some cases that are needed for remedial actions (Barpi, F.and Valente, S., 2008).

4.1.1 Density of Concrete Material

CEB-FIP (1991) gives a mean value of 23.5 kN/m^3 with a standard deviation of 0.940 kN/m^3 or the coefficient of variation (COV) of 0.04 for concrete of compressive strength 20 MPa, and 24.5 kN/m^3 with a standard deviation of 0.735 kN/m^3 or COV = 0.03 for concrete of compressive strength greater than 40 MPa.

4.1.2 Friction Angle and Cohesion Parameters of Concrete to Rock and Concrete to Concrete Interface

In the absence of test data, Category III rock mass of medium sound with the friction angle, f with the value of 45.0^o and cohesion, C with their standard deviations, is based on the China Electric Council (2010) recommendation has been assumed for the rock-concrete interface at the foundation level. Table 1 indicates the friction angle parameters of concrete- rock interface at the foundation level.

Table 1 Friction angle parameters of concrete to rock interface.

Rocks properties of dam foundation	Friction angle, f ^{o}		Cohesion, C (MPa)	
	Mean	Standard Deviation, s	Mean	Standard Deviation, s
Category I: dense and sound, the distance between cracks > 1 m	56.31 52.43	16.70 14.57	1.5 1.3	0.54 0.47
Category II: sound, weakly weathered massive rock with crack spaces distance between 0.5-1m	52.43 47.73	14.57 11.86	1.3 1.1	0.47 0.40
Category III: Rock mass of medium sound with crack spaces distance between 0.3-0.5m	47.73 41.99	11.86 11.31	1.1 0.7	0.40 0.28

4.2 Load Cases

The load case events adopted in the analyses are as follows;

1. S1- Usual Load Case: Full supply level (FSL)
2. S2- Unusual Load Case: Design Flood Level (DFL)
3. S3- Extreme Load Case: Overturning Level (OL)

The uplift drainage cases are as follows;

1. D1 - Normal Drainage (100% drainage efficiency)
2. D2 - Extreme Drainage (0% drainage efficiency)

The tail water level and silt level at FSL, DFL and OL is 5.00 m and 13.3m respectively.

The reliability-based using FORM-Taylor Series Approximation and Monte Carlo Simulation (MCS) are carried out based on the above conditions to determine the probability of failure for the sliding and overturning failure modes that are applied to the gravity concrete dam main section. Mitigation measures with various options are carried out using a more accurate Monte Carlo analysis.

5 Methodology

Two methods of reliability risk analysis - the simplified FORM with Taylor Series approximation and Monte Carlo analysis - have been used in this paper. The first Taylor Series method is a probabilistic simplified analysis, though somewhat less precise, and was used by USACE (1997 and 1998) and Duncan (2000). The second Monte Carlo Simulation (MCS) probabilistic analysis was carried out using a 10 million sample population provides a more rigorous and precise form of analysis than the FORM-Taylor Series method. The mitigation measure options are included in the MCS probabilistic analysis.

5.1 Reliability-based analysis using FORM-Taylor Series Approximation.

A simplified reliability analysis using the FORM-Taylor series approximation as proposed by Duncan (2000) is carried out for the RCC concrete dam for the stability checks against sliding and overturning, mathematically simpler, though somewhat less precise but adequate for design practice, that can be performed using excel spreadsheet.

The terms involved in computing the sliding factor of safety FOS [$W_{concrete}$, tan f] and overturning factor of safety FOS [$W_{concrete}$] all involve some degree of uncertainty. Therefore, the computed value of the sliding and overturning factor of safety also involves some uncertainty. It is useful to be able to assess the Reliability of sliding and overturning factors of safety, as well as the best estimate of its value.

The calculation steps using the reliability-based FORM-Taylor Series approximation are as follows:

Step 1. Determine the most likely values of the parameters involved and compute the factor of safety by the normal (deterministic) method for sliding and overturning. This is sliding F_{MLV} or overturning F_{MLV}.

$$Sliding\ F_{MLV} = \frac{\{CA + (\sum W_{conc} + \sum W_{water} + \sum W_{silt} - \sum U_{uplift}) \tan \emptyset\}}{F_h + F_{silt} - F_{tail}} \quad (8)$$

$$Overturning\ F_{MLV} = \frac{\{\sum W_{conc} \cdot x_{conc.} + \sum W_{water} \cdot x_{water} + \sum W_{silt} \cdot x_{silt} + F_{tail} \cdot \frac{h_{tail}}{3}\}}{F_h \cdot \frac{h_w}{3} + F_{silt} \cdot \frac{h_{silt}}{3} + \sum U_{uplift} x_u} \quad (9)$$

The above deterministic analysis using the above factor of safety can be easily extended into the first-order reliability analysis using first-order Taylor Series approximation.

Step 2. Estimate the mean and standard deviations of the parameters that involve uncertainty. i.e., angle of friction, f and density of concrete, g_{conc} are considered as random variables with normal distributions.

1. CEB-FIP (1991) gives the concrete density, g_{conc} of a mean value of 24.5 kN/m^3 with a standard deviation, s of 0.735 kN/m^3 for concrete of compressive strength of 40 MPa.
2. China Electric Council (2010) Category III rock mass of medium sound with a friction angle value, f of 45.0^o and standard deviation of 11.5^o and cohesion, C of 0.91 MPa with s a value of 0.34 MPa were used for the concrete dam foundation concrete-rock interface.

Step 3. Use the Taylor series technique (Wolff, 1994; USACE 1997, 1998 and Duncan, 2000) to estimate the standard deviation and the coefficient of variation of the factor of safety using these formulas:

$$\sigma_F = \sqrt{(\frac{\Delta F1}{2})^2 + (\frac{\Delta F2}{2})^2} \quad (10)$$

$$V_F = \frac{\sigma_F}{F_{MLV}} \quad (11)$$

Calculate the safety factor by varying each parameter upwards by one standard deviation and then downwards by one standard deviation from the mean value while maintaining the other parameters at their most probable values. This process produces N values for F^+ and N values for F^-. Using these F^+ and F^- values, calculate their differences, denoted as ΔF, for each parameter. Subsequently, the standard deviation of the factor of safety (σ_F) is determined through equation (7), and the coefficient of variation of the factor of safety (V_F) through equation (8). To calculate β, the First Order Reliability Method (FORM) method uses a Taylor series expansion as above, simplified by using only the first term (hence, "First Order").

Step 4. Use an Excel spreadsheet to determine the value of FMLV from the first step and the value of VF from the third step to determine the value of Pf. The key to computing more precise values of P_f is to compute the value of the lognormal reliability index, b_{LN}, using the following formula (Scott et al. 2001):

$$b_{LN} = \frac{ln\,(F_{MLV}/\sqrt{1+V^2}}{\sqrt{ln(1+V^2)}} \quad (12)$$

where b_{LN} = lognormal reliability index; V = coefficient of variation of a factor of safety; and F_{MLV} = most likely value of factor of safety.

Step 5 When b_{LN} has been computed using (9), the value of P_f can be determined accurately using the built-in function NORMSDIST in Excel. The argument of this function is the reliability index, b_{LN}. In Excel, under "Insert Function," ''Statistical,'' choose ''NORMSDIST,'' and type the value of b_{LN}.

Step 6 Check the value of sliding and overturning mode of failure P_f < set value of 10^{-4} or 10^{-5} as required by ICOLD Tolerable Risk Guidelines.

5.2 Reliability-based analysis using Monte Carlo Simulation

A practical alternative is to develop probability distributions for the various parameters and apply a more rigorous MCS with a higher degree of accuracy to determine the probability that the actual safety factor is below some threshold value associated with instability or other types of bad performance.

The Monte Carlo analysis is coded in Matlab for the concrete gravity dams with the mitigation measures, and its basic calculation steps are listed below:

- Step 1 Build a probabilistic model of limit state analysis for a safety factor for sliding and overturning moment as given in Equation 5 and Equation 6.
- Step 2 Assign the mean and probability distributions to the model inputs for uncertainty in material properties, i.e., density of concrete, g_{conc} of 24.5 kN/m^3, friction angle, 45.0o and cohesion, and Cu of 0.91 MPa. The concrete density value is based on CEB-FIP (1991) and China Electric Council (2010) Category III rock mass of medium sound for the angle of friction and cohesion.
- Step 3 Sample the model inputs based on their normal distributions and constraints using the 3-sigma rule.
- Step 4 Input all the constant or determinate values.
- Step 5 Run the model for the safety factor for sliding and overturning.
- Step 6 Record the model output factor of safety.
- Step 7 Repeat for the specified samples of the model inputs. 10 million input samples are used in this case.
- Step 8 Compute the number of samples with the factor of safety < 1.0; however, the safety factor is a constraint to be greater than zero.
- Step 7 Evaluate the probability distribution for the model outputs with N=10^6.

$$P_f = \frac{1}{N}\sum_{i=1}^{N} I[X_i] = \frac{N_f}{N} \quad (13)$$

Probability of Failure = No of samples with the factor of safety < 1.0 / Total No of Samples.

Matlab Code for Sliding Mode of Failure

```
for i=1:MCS_Sample

W_Concrete(i) =
Area_of_Concrete*Density_of_Concret
e_distribution(i);

Sliding_FOS(i) =
((Cohesion_distribution(i)*Area_of_
Contact+((W_Concrete(i)+W_Water+W_S
ilt-Total_Uplift_Force)
*tand(Friction_Angle_distribution(i
)))))
/((Horizontal_Hydraulic_Force_Upstr
eam+Horizontal_Force_Silt-
Horizontal_Hydraulic_Force_Downstre
am));

end

FOS_Below_One = nnz(Sliding_FOS<1);
Probability_of_Failure =
FOS_Below_One/MCS_Sample;
```

Matlab Code for Overturning Mode of Failure

```
for i=1:MCS_Sample

        W_Concrete(i) =
    Volume_of_Concrete*Density_of_Conc
    rete_distribution(i);

   Overturning_FOS(i) =
(Cohesion_distribution(i)*Area_of_Conta
ct+(W_Concrete(i)*Lever_arm_Xconcrete)+
(W_Water*Lever_arm_Xwater)+(W_Silt*Leve
r_arm_Xsilt))/((Horizontal_Hydrostatic_
Force_Upstream*Lever_arm_Ywater_Upstrea
m)+(Horizontal_Force_Silt*Lever_arm_Ysi
lt)+Total_Uplift_Moment-
(Horizontal_Hydrostatic_Force_Downstrea
m*Lever_arm_Ywater_Downstream));

end

FOS_Below_One = nnz(Overturning_FOS<1);
Probability_of_Failure =
FOS_Below_One/MCS_Sample;
```

- Step 8 Calculate the Reliability Index, b. Set b > 8 if the number of samples with a factor of safety < 1.0 is zero with a probability of failure = 0.
- Step 9 Display the output and plot the graph of the number of samples against the safety factor.
- Step 10 If the value of sliding mode of failure P_f > set

value as required by ICOLD(2005) or USBR-USACE(2019) Tolerable Risk Guidelines, then go to Step 11 for mitigation measures for Option 1 Post-Tensioned Anchors and Option 2 Horizontal Load on Piles.

- Step 11. The performance function for the sliding F_{MLV} with its mitigation Option 1 and Option 2 are as follows;

Option 1 - Post Tensioning, Post Tensioned Forces (Vertical Pv and Horizontal Ph) usually set at 45° angle from the vertical axis.

$$Sliding\ F_{MLV} = \frac{\{CA + (\sum W_{conc} + \sum W_{water} + \sum W_{silt} + Pv - \sum U_{uplift}) \tan \emptyset\}}{F_h + F_{silt} - F_{tail} - Ph} \quad (14)$$

Matlab Code for Mitigation Measures - Option 1 Post-tensioning

```
for i=1:MCS_Sample

    W_Concrete(i) =
Area_of_Concrete*Density_of_Concrete_
distribution(i);

    Sliding_FOS(i) =
((Cohesion_distribution(i)*Area_of_Co
ntact)+((W_Concrete(i)+W_Water+W_Silt
+Vertical_Posttension_Force-
Total_Uplift_Force)*tand(Friction_Ang
le_distribution(i))))/(Horizontal_Hyd
raulic_Force_Upstream+Horizontal_Forc
e_Silt-
Horizontal_Hydraulic_Force_Downstream
-Horizontal_Posttension_Load);

end

FOS_Below_One = nnz(Sliding_FOS<1);
Probability_of_Failure =
FOS_Below_One/MCS_Sample;
```

Option 2 - Horizontal Load (H) on Piles at the toe.

$$Sliding\ F_{MLV} = \frac{\{C_u A + (\sum W_{conc} + \sum W_{water} + \sum W_{silt} - \sum U_{uplift}) \tan \emptyset\}}{F_h + F_{silt} - F_{tail} - H} \quad (15)$$

Matlab Code for Mitigation Measures - Option 2 Raked Micro-pile

```
for i=1:MCS_Sample

    W_Concrete(i) =
Area_of_Concrete*Density_of_Concrete_distri
bution(i);

    Sliding_FOS(i) =
((Cohesion_distribution(i)*Area_of_Contact)
+((W_Concrete(i)+W_Water+W_Silt -
Total_Uplift_Force)*tand(Friction_Angle_dis
tribution(i))))/(Horizontal_Hydraulic_Force
_Upstream+Horizontal_Force_Silt-
Horizontal_Hydraulic_Force_Downstream-
Horizontal_Load);

end

FOS_Below_One = nnz(Sliding_FOS<1);
Probability_of_Failure =
FOS_Below_One/MCS_Sample;
```

Step 12 Loop into Steps 5, 6, 7, 8, and 9.

Step 13 If the value of sliding mode of failure $P_f <$ set value, i.e. 10^{-4} or 10^{-5} or 10^{-6} as required by ICOLD Tolerable Risk Guidelines, print the Horizontal Load on Pile H for Option 1 and Post Tensioned Force P_v and P_h for Option 2.

The typical output file for MCS without and with mitigation measures for Option 1 Post-Tensioned at 45° and Option 2 Horizontal Load on Pile for S1 Full Supply Level event scenario with D2 Extreme Uplift condition for a probability of failure of 10^{-5} is given in Appendix 1.

6 Results and discussion

The two predominant probabilities of failures – sliding and overturning modes - main body section of the concrete gravity dam is being analysed and discussed in this section.

6.1 Factor of Safety, Probability of Failure, and Reliability Index Concrete-Foundation Level

The summary of the results for the sliding factor of safety, reliability index, and probability of failure using the FORM-Taylor Series and MCS probability of failure is shown in Table 2.

The above sliding factor of safety for full supply level (FSL), design flood level (DFL), and overtopping level (OL) for both normal and extreme uplift are greater than the minimum sliding factor of safety for usual, unusual, and extreme flood is 1.5, 1.3 and 1.1 respectively as per Table C.8 of MyDAMS (2017).

The FSL under the D1 condition has the highest sliding reliability index of b_{TS} FORM-Taylor = 1.598 or b_{MCS} =1.844, while OL under the D2 condition has the lowest value of b_{TS} FORM-Taylor Series = 0.934 or b_{MCS} =0.986.

The summary of the results for the overturning factor of safety and probability of failure is shown in Table 3.

Table 2: Sliding Factor of Safety, Reliability Index, and Probability of Failure

			D1 Normal Uplift - 100% Efficiency			**D2 Extreme Uplift - 0% Efficiency**		
Event Scenario	h_w (m)	h_{tail} (m)	Sliding F_{MLV}	Taylor Series $P_{fTS}(b_{TS})$	Monte Carlo $P_{fMCS}(b_{MCS})$	Sliding F_{MLV}	Taylor Series $P_{fTS}(b_{TS})$	Monte Carlo $P_{fMCS}(b_{MCS})$
S1 Full Supply Level - FSL	38	5	2.05	5.497E-02 (1.598)	3.25574E-02(1.844)	1.85	8.884E-02 (1.348)	5.33451E-02 (1.342)
S2 Design Flood Level-DFL	40	5	1.85	9.056E-02 (1.337)	5.39335E-02 (1.607)	1.66	1.425E-01 (1.069)	8.92142E-02 (1.346)
S3 Overtopping Level - OL	41	5	1.76	1.128E-01 (1.212)	6.83949E-02 (1.488)	1.57	1.750E-01 (0.934)	1.621013E-01(0.986)

Notation: h_w is upstream head of water, h_{tail} is downstream tail head of water, and P_f Probability of Failure and b Reliability Index is given in bracket.

Table 3: Main Body Section - Overturning Factor of Safety and Probability of Failure P

			D1- Normal Uplift (100% Efficiency)			**D2-Extreme Uplift (0% Efficiency)**		
Event Scenario	h_w (m)	h_{tail} (m)	Overturn -ing F_{MLV}	Taylor Series P_f	Monte Carlo P_f	Overturn -ing F_{MLV}	Taylor Series P_f	Monte Carlo P_f
S1 Full Supply Level (FSL)	38	5	1.92	0.000E+00 (26.439)	0.000E+00 (>8)	1.72	0.000E+00 (16.023)	0.000E+00 (>8)
S2 Design Flood Level (DFL)	40	5	1.78	0.000E+00 (23.625)	0.000E+00 (>8)	1.59	0.000E+00 (13.240)	0.000E+00 (>8)
S3 Overtopping Level (OL)	41	5	1.71	0.000E+00 (22.220)	0.000E+00 (>8)	1.54	0.000E+00 (11.853)	0.000E+00 (>8)

Notation: hw is upstream head of water, htail is downstream tail head of water, and Pf Probability of Failure

The FSL under D1 has the highest overturning reliability index (b_{TS} FORM-Taylor Series = 26.439, b_{MCS} >8), and OL under D2 Extreme Uplift condition has the lowest (b_{TS} FORM-Taylor Series = 11.853, b_{MCS} > 8).

In the MCS, the number of samples run is 10 million and zero failure is recorded when b > 7.87375 i.e., P_f = 00.000E+00. In the MATLAB coding for MCS, the operational limit where no probability of failure occurs is set at b > 8 in Table 3. There is no probability of overturning failure (P_{fTS} = 00.000E+00, P_{fMCS} = 00.000E+00 for all the events under FSL, DFL, and OL with both D1 and D2 conditions.

Fig. 4 indicates the sliding factor of safety and reliability index b for the FORM-Taylor Series and MCS.

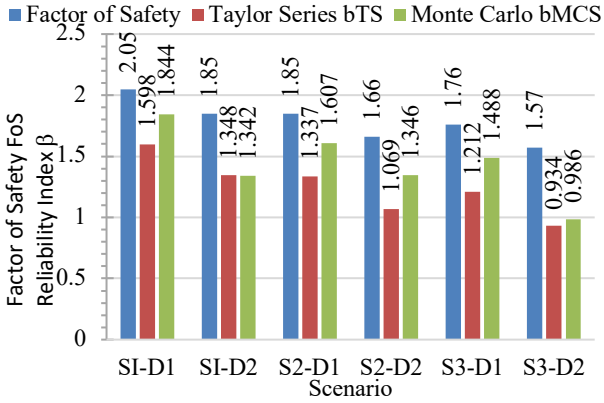

Fig. 4: Sliding Factor of Safety and Reliability Index

The factor of safety for sliding follows the same trendline as the reliability index, b_{TS} of FORM-Taylor Series and b_{MCS} of MCS. b_{MCS} values of MCS are slightly higher than b_{TS} values of the FORM-Taylor Series.

Fig. 5 indicates the overturning factor of the safety and reliability index b for the FORM-Taylor Series and MCS.

The factor of safety and reliability index decreases for each drainage condition (D1 and D2) as the scenario events (S1, S2 and S3) change with their load cases from lower to higher headwater levels. No direct comparison can be made between the reliability index, b_{TS} for FORM-Taylor Series and b_{MCS} for MCS. In the MATLAB coding for MCS, the operational limit where no probability of failure occurs is set as b > 8 i.e P_f = 00.000E+00.

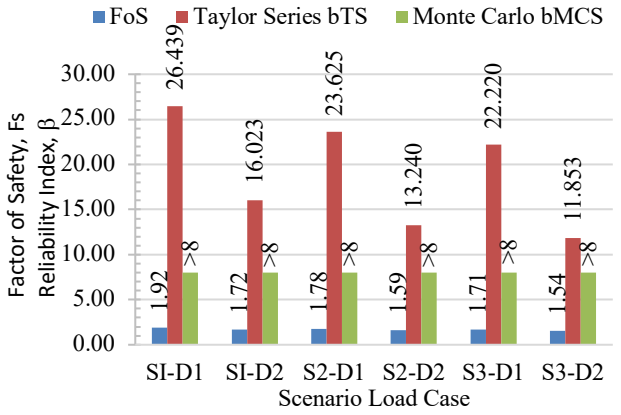

Fig. 5: Overturning Factor of Safety and Reliability Index b

Fig. 6 shows the relationship between the probability of failure P_f and sliding factor of safety, F_s for FORM-Taylor Series and MCS.

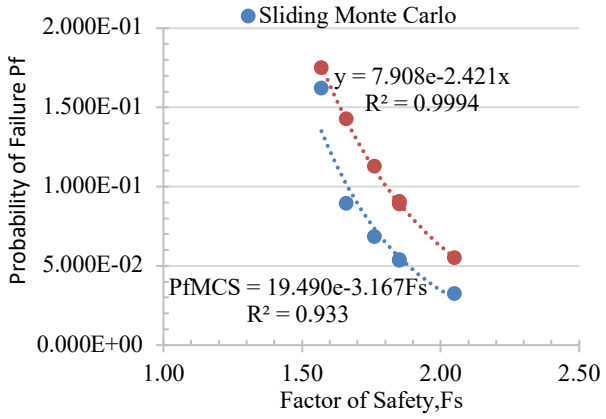

Fig. 6: Relationship between Sliding Probability of Failure P_f and Factor of Safety, F_s

The results indicate an excellent exponential correlation between the probability of failure P_f and sliding factor of safety, Fs for FORM-Taylor Series and MCS with $R^2 > 0.933$ the following relationship;

- FORM-Taylor Series $P_{fTS} = 7.908e^{-2.421Fs}$ with $R^2 = 0.9994$
- Monte Carlo Simulation $P_{fMCS} = 19.490e^{3.167Fs}$ with $R^2 = 0.933$

The probability of failure of P_f decreases exponentially with the increase in the safety factor, F_S, for both the FORM-Taylor Series and Monte Carlo analysis. The FORM-Taylor Series, P_{fTS} is higher than the Monte Carlo probability of failure P_{fMCS} for the given sliding factor of safety.

Fig. 7 shows the sliding probability of failure P_f for FORM-Taylor Series and MCS and their normalized values.

Interestingly, the risk probability of failure for the S2-D2 event is higher than S3-D1 due to the higher D2 extreme uplift condition in S2-D2 against the higher headwater effect with D1 normal uplift for S3-D1. The normalized FORM-Taylor to MCS probability of failures P_f values ranges from 1.08 to 1.76 with an average value of 1.58. Generally, the FORM-Taylor probability of failure is more conservative than the MCS value except for the S3-D2 scenario, which is only 8% higher.

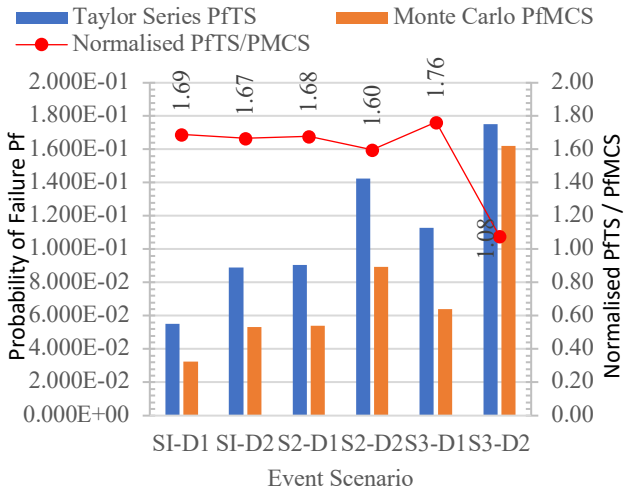

Fig. 7: Sliding Probability of Failure, P_f and Normalized Values Taylor Series-Monte Carlo

Fig. 8 illustrates the relationship between the FORM-Taylor Series and MCS probability of failure.

The results indicate a good linear correlation between the FORM-Taylor Series, P_{fTS}, and Monte Carlo analysis P_{fMCS} for sliding with $R^2 = 0.9542$ with the following relationship;

$$P_{fTS} = 1.3227\, P_{fMCS}$$

FORM-Taylor Series, P_{fTS} values are generally 1.3227 times or 32.3% more conservative than MCS P_{fMCS} for sliding, as given in the above correlation equation. Thus, FORM-Taylor probability values can be safely used at the preliminary stage; however, a more accurate MCS is required in the design, construction, and rehabilitation stage to evaluate the risk on the probability of failure.

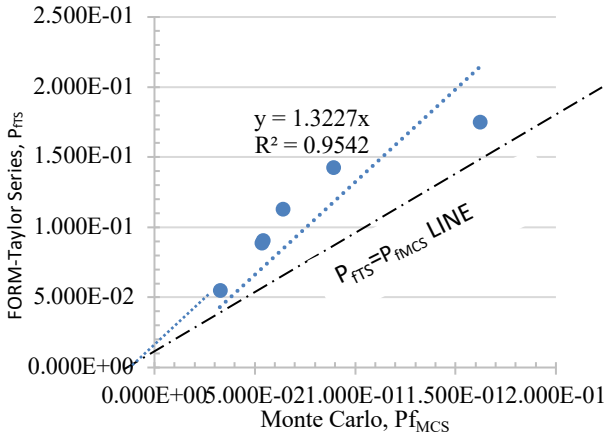

Fig. 8: Sliding Probability of Failure – Correlation between FORM-TS and MCS

No direct comparison can be made between the reliability index, b_{TS} for FORM-Taylor Series, and b_{MCS} MCS. In the MATLAB coding for MCS, the operational limit where no probability of failure occurs is set at $b > 8$, i.e., P_f = 00.000E+00.

From the reliability analysis, the sliding failure mode was the dominant mode over the overturning mode of failure. The most probably been friction angle is the most influential random variable in this failure mode. The overturning had a significantly lower probability of occurrence than sliding. The overturning modes had a very low probability of occurrence, with the reason being that the stabilizing Weight of concrete with only a negligible destabilizing uplift force for the buttress dam.

A probabilistic model applying FORM analysis is advantageous when seeking more accurate sensitivity studies and recommending its use with MCS. If a calculation model of limit equilibrium using MCS may not be assessable for a small consulting firm, a probabilistic model applying FORM-Taylor analysis may be the most viable option but may jeopardize the accuracy of the construction and mitigation measures.

6.2 Sensitivity Analysis

Sensitivity analysis explores how sensitive the output variables are to the uncertainties in the input variables. Sensitivity analysis is particularly important in risk decision-making that relies on complex models, as it provides insights into the model's reliability when faced with uncertainties in input data. Table 4 indicates the sensitivity analysis on the independent input variable friction angle, cohesion and concrete density for sliding. However, no sensitivity analysis is performed for overturning as it has only one input variable, i.e., concrete density. DF values measure the swing on the factor of safety for the angle of friction, f^o, cohesion, C, and the density of concrete, g_{conc} was taken from the FORM-Taylor Series analysis spreadsheet for sliding.

The friction angle, f^o swing DF, ranges from 1.30 to 1.70 with an average of 1.482, cohesion, C swing DF, is constant at 0.003, and density of concrete, g_{conc} swing DF, ranges from 1.13 to 1.15 with an average of 1.14.

Fig. 9 indicates the pie-chart sensitivity analysis on the independent input variable friction angle, cohesion, and concrete density for sliding given in percentage. The sensitivity for the friction angle is 91.2%, concrete density is 8.6%, and cohesion is 0.2%. It can be seen that the friction angle is very sensitive, and the density of concrete is less sensitive, while cohesion has little effect on the sliding mode of failure.

It is prudent to have extensive field data on the friction angle, f^o at the design and construction stage. In this sense, the Taylor Series Method can be viewed as a structured sensitivity analysis or parametric study that may be required to prioritize the geotechnical investigation works at the site.

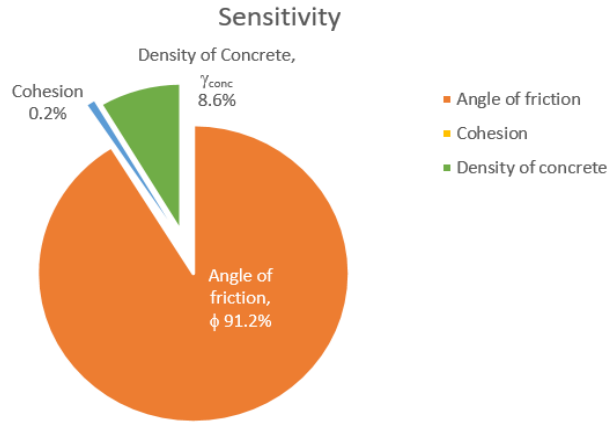

Fig. 9: Sensitivity Analysis for Sliding

6.3 Mitigation Measures using Monte Carlo Reliability Risk Analysis

A highly accurate MCS should be used more than the FORM Taylor Series at the mitigation stage for strengthening works.

The overturning mode has no probability of failure for all scenario events of load cases; as such is not a critical failure mode for the dam. Sliding is the most dominant mode of failure, and the probability of failure is higher than $10^{-4,}$ which is not in compliance with ICOLD (2005) and USBR-USACE (2019) requirements.

The dam strengthening options which deemed feasible for mitigation measures for the sliding mode of failure were based on the three (3) options as follows;

1. Option 1 New permanent post-tensioned ground anchors at the dam downstream face
2. Option 2 Raked micro-piles at the dam toe
3. Option 3 Mass concrete buttressing on the downstream side of the dam

Typical arrangements for the three dam strengthening options are shown in Fig. 10. Option 1 and 2 were the most

viable option in the mitigation measures due to cost, operation, and time effectiveness. Option 3, with mass concrete buttressing on the downstream side toe, is not included to proceed to detail design due to the increase in the footprint of the dam, which required the demolition of the outlet pipe and construction of a new outlet structure downstream that will interrupt the operational requirements of the existing dam. Lateral load on vertical micro-piles as an alternative for Option 2 can also be considered; however, only raked micro-piles are investigated in this study. For existing dams, the individual risk to the identifiable person or group, defined by a location most at risk, should be less than a limit value of 1 in 10,000 or 10^{-4} per year (ANCOLD, 2003).

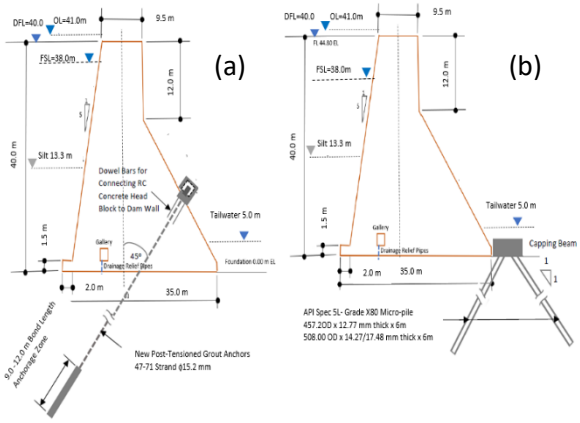

(a) Option 1 New Post-Tensioned

(b) Option 2 Raked Micro-piles at the dam toe

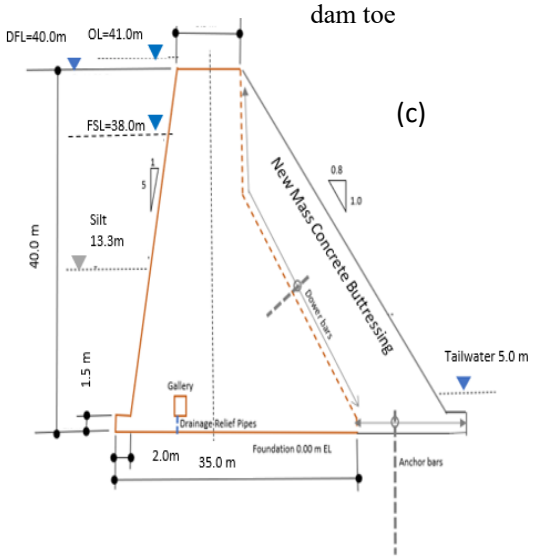

(c) Option 3 Mass concrete buttressing on the downstream side toe

Fig. 10: Dam Strengthening Options

Table 4: Sensitivity Analysis for Sliding

Input	FSL - Swing DF		DFL - Swing DF		OL - Swing DF		Aver-age	Sensit-ivity
Variable	S1-D1	S1 -D2	S2-D1	S2 -D2	S3-D1	S3 -D2	Swing DF	%
The angle of friction, f^o	1.70	1.53	1.53	1.37	1.46	1.30	1.482	91.2
Cohesion, C	0.003	0.003	0.003	0.003	0.003	0.003	0.003	0.2
Concrete Density, g_{conc}	0.15	0.15	0.14	0.14	0.13	0.13	0.14	8.6

However, under the Dam Risk Matrix of USBR-USACE (2019), when the loss of life is 10 with a Level 2 consequence, the loss of life is 100 with a Level 3 consequence, and the loss of life is 1000 with a Level 4 consequence, the probability of failures needs to be less than 10^{-4}, 10^{-5} and 10^{-6} respectively. Table 5, Table 6, and Table 7 are tabulated based on the above probability of failure criterion.

Table 5 shows the probability of failure using Monte Carlo Simulation (MCS) for the mitigation measures for Option 1 and Option 2 to meet the ICOLD (2005) and USBR-USACE (2019) P_f criterion of 10^{-4}, 10^{-5} and 10^{-6} requirements.

At each FSL, DFL, and OL scenario for Option 1, the post-tensioned load increases marginally by only 2.8-3.5% for D1 and D2 drainage conditions if the probability of failure needs to decrease from 10^{-4} to 10^{-6}. As such, lowering risk tolerability from 10^{-4} to 10^{-6} has only a minor cost impact for each scenario. However, if the probability of failure needs to meet the probability criterion of less than 10^{-4}, $10^{-5,}$ and 10^{-6} from S1 to S3 events for both D1 and D2 drainage conditions, the post-tensioned load needs to be increased by 17.0-18.8%, 16.6-18.6%, and 11.6-18.3% respectively.

At each FSL, DFL, and OL scenario for Option 2, the horizontal load on piles increases marginally by only 3.0-3.7% for D1 and D2 drainage conditions if the probability of failure needs to decrease from 10^{-4} to 10^{-6}. As such, lowering risk tolerability from 10^{-4} to 10^{-6} has only a minor cost impact for each scenario. However, if the probability of failure needs to meet the probability criterion of less than 10^{-4}, $10^{-5,}$ and 10^{-6} from S1 to S3 for both D1 and D2 drainage conditions, the horizontal load needs to be increased by 16.8-19.0%, 16.6-18.4%, and 11.6-18.2% respectively.

6.3.1 Post-tensioned Anchors

High-capacity, post-tensioned anchors have found widespread use, originally in initial dam design and construction and more recently in the strengthening and rehabilitating of concrete dams to meet modern design and safety standards. Brown (2015) has extensively reviewed the rock engineering design of post-tensioned anchors for dams. Each anchor would comprise 7-wire super grade steel strands of 15.2mm diameter, with a minimum breaking load (MBL) of 265kN. The post-tension anchors have adopted a working load of 0.60MBL per strand. Current post-tensioned ground

anchors are redressable

Table 5: Mitigation Measure for Option 1 and Option 2 – Scenario, Forces, and Probability of Failure

Scenario	USBR-USACE (2019) P_f Criterion	**Option 1 Post Tensioned at 45° - $P_{45°}$ (kN/m run)**						**Option 2 Horizontal Load on Pile - H (kN/m)**			
		D1- Normal Drainage			D2- Extreme Drainage			D1- Drainage		D2- Drainage	
		$P_V = P_H$	$P_{45°}$	P_f	$P_V = P_H$	$P_{45°}$	P_f	H	P_f	H	P_f
S1 Full Supply Level (FSL)	$\leq 10^{-4}$	2960	4186	1.04E-04	3250	4596	1.00E-04	3704	1.02E-04	4064	1.05E-04
	$\leq 10^{-5}$	3070	4342	1.02E-05	3355	4745	1.05E-05	3834	1.03E-05	4201	1.02E-05
	Nil	3180	4497	0.00E+00	3460	4893	0.00E+00	3964	0.00E+00	4338	0.00E+00
S2 Design Flood Level (DFL)	$\leq 10^{-4}$	3584	5069	1.02E-04	3890	5501	1.02E-04	4488	1.06E-04	4870	1.05E-04
	$\leq 10^{-5}$	3690	5218	1.02E-05	3998	5654	1.00E-05	4618	1.03E-05	5010	1.03E-05
	Nil	3796	5368	0.00E+00	4106	5807	0.00E+00	4748	0.00E+00	5150	0.00E+00
S3 Overtopping Level (OL)	$\leq 10^{-4}$	3906	5524	1.01E-04	5067	7166	9.70E-05	4890	1.01E-04	6350	1.03E-04
	$\leq 10^{-5}$	4020	5685	1.04E-05	5189	7338	1.01E-05	5030	9.90E-06	6492	1.05E-05
	Nil	4134	5846	0.00E+00	5311	7511	0.00E+00	5170	0.00E+00	6634	0.00E+00

Table 6: Option 1 Post-tensioned Anchor Requirements – Design Load and Probability of Failure

	Option 1 New Post-tensioned Anchor @ 1.5m spacing									
Scenario	USBR-USACE (2019) P_f Criterion	Anchor Groups ID	Required Design Load (kN)	Range No of Strands	Design Capacity Range, Tc (kN)	Selected No of Strands[1]	Design Load (60% Tc) (kN)	Hole size (mm)	Cable bond Length (m)	Anchor Spacing
FSL (S1-D1& S1-D2)	$<10^{-4}$	A1	6894	44-45	11660 - 11925	44	6996	300	10	1.5m
	$<10^{-5}$	A2	7118	45-46	11925 - 12190	45	7155	300		
	Nil	A3	7340	46-47	12190 - 12455	47	7473	300		
DFL (S2-D1& S2-D2)	$<10^{-4}$	B1	8251	50-52	13250 - 13780	52	8268	350	10	1.5m
	$<10^{-5}$	B2	8481	53-55	14045 - 14575	55	8745	350		
	Nil	B2	8711	53-55	14045 - 14575	55	8745	350		
OL (S3-D1& S3-D2)	$<10^{-4}$	C1	10749	69-70	18285 - 18550	69	10971	350	12	1.5m
	$<10^{-5}$	C2	11007	69-70	18285 - 18550	70	11130	350		
	Nil	C3	11267	70-71	18550 - 18815	71	11289	350		

Note 1: 7 wire super strand- 15.2 mm diameter of 143mm2 area with a minimum breaking load =265 kN

Table 7: Option 2 Micro-pile Capacity Requirements – Design Load and Probability of Failure

Scenario	USBR-USACE (2019) P_f Criterion	**Option 2 Raked Pile Load (kN) @1.5 m spacing**						API Pile (OD x Thick x length)	API Pile Capacity, P at 1.5 m spacing
		D1- Normal Drainage			D2- Extreme Drainage				
		H	P_f	Compression= Tension	H	P_f	Compression= Tension	(mm)	(kN)
Full Supply Level - S1	$\leq 10^{-4}$	5566	1.08E-04	3936	6096	9.02E-05	4311	457.2 OD x 12.77 x 6000	4895
	$\leq 10^{-5}$	5751	1.02E-05	4067	6302	1.03E-05	4456		
	Nil	5946	0.00E+00	4204	6761	0.00E+00	4781		
Design Flood Level - S2	$\leq 10^{-4}$	6732	1.04E-04	4760	7305	9.09E-05	5165	508.00 OD x 14.27 x 6000	6109
	$\leq 10^{-5}$	6927	1.04E-05	4898	7515	1.04E-05	5314		
	Nil	7122	0.00E+00	5036	7725	0.00E+00	5462		
Overtopping Level - S3	$\leq 10^{-4}$	7355	1.00E-04	5201	9525	1.05E-04	6735	508.00 OD x 17.48 x 6000	7435
	$\leq 10^{-5}$	7545	1.05E-05	5335	9738	1.03E-05	6886		
	Nil	7755	0.00E+00	5484	9951	0.00E+00	7036		

and protected against corrosion by greased sheaths with an expected design life of 100 years. An ultimate grout-rock bond strength is 1.5-2.5MPa, where the foundation is assumed as weathered granite with joints spaced between 0.3m (BS8081, 2015; Littlejohn, 1992; Littlejohn, 1993). Following the procedure, the cable bond length has been proportioned for the design working load in the anchor (60% MBL) with a minimum safety factor of 2 on the above-average ultimate bond strength of 2.0 MPa. This approach produces a required bond length of 10.0 m – 12.0 m for the anchors depending on the required design load of each event scenario.

Table 6 shows the Option 1 post-tensioned anchor requirements to meet the mitigation design loads and its probability of failure criterion.

If the probability of failure needs to be decreased from 10^{-4} to no failure for each FSL, DFL, and OL event scenario, the post-tensioned design load needs to increase marginally only by 4.8 - 6.5% with a minor additional strand of 2-3 numbers. As such, lowering risk tolerability from 10^{-4} to no failure has a negligible cost and time impact. Practically, there are no changes for the number of post-tensioned strands required, with no change in the cost if the probability of failure needs to be decreased from 10^{-5} to no likelihood of failure.

If the existing dam needs to be designed for no likelihood of failure under a DFL event, the number of post-tensioned strands needed is 55. However, if the existing dam needs to be designed for no likelihood of sliding failure under all the event scenarios, the number of post-tensioned strands needs to be changed from 55 to 71. These additional 16 strands may have only a minor impact on the construction cost and time.

6.3.2 Raked Micro-piles

Micro-piles using API pipes have been generally accepted as a cost-effective, reliable, environmentally friendly piling system for retrofitting foundations.

Structural Working Capacity, $P = A_s \times s_y/FoS$

Whereas is the area of API pipe, s_y is the minimum yield strength of 552 N/mm2 for API Spec 5L- Grade X80, and the factor of safety (FoS) is usually taken as 2.0.

Allowable Geotechnical Capacity, $Q_a = At_{ult.\ bond} / FoS$

Where A is the surface area of the bond, $t_{ult,\ Bond}$ is the ultimate bond strength is 2 MPa for weathered granite to Table B.2 of BS8081:2015 with an FoS =2. This approach produces a socketed length ranging from 3.4 m to 4.7 m. In a highly fractured rock, it is recommended to use a minimum socketed length of 5.0m. Adopt a micro-pile of the minimum length of 6m long with a 5.0 m rock socketed length.

Table 7 shows the Option 2 micro-pile capacity requirements to meet the mitigation design loads and its probability of failure criterion.

If the probability of failure needs to decrease from 10^{-4} to no likelihood of failure for each FSL, DFL, and OL scenario, the micro-pile axial load capacity increases marginally by 3.0-3.7% only under D1 and D2 drainage conditions with no changes in size and length of the micro-pile are involved. Practically, there are no changes in construction cost and time.

If the existing dam needs to be designed for no likelihood of sliding failure under all the event scenarios, the API pile needs to be changed from 457.2OD x 12.77 mm thick to the next 508.00OD x 17.48 mm thick size of the same length. This next size requirement has a minor impact on the cost and time of construction.

Operation-wise and design risk impact, Option 2 is better than Option 1. Option 1 may weaken the body of the dam structure when coring through the dam is involved, and the dam may not be able to operate under normal supply conditions without the design and operational risk. Further, Option 1 may warrant more coordination works at the site during construction. Option 2 did not intrude into the main body of the structure and did not interfere with the operation of the existing hydropower plant.

Reliability risk analysis using Monte Carlo simulation is a powerful tool that can be utilized in the assessment and mitigation measures of the existing dam under different event scenarios and remedial options study to comply with the required tolerable risk guidelines such as ICOLD (2005) and USBR-USACE (2019). The output from the analysis can be directly used to design the detailed elements of the mitigation options.

7 Conclusions

1. Monte Carlo simulation provides a more accurate reliability risk analysis, and it is advisable to be used at the mitigation stage than the FORM-Taylor Series approximation, which is more conservative. FORM-Taylor Series approximation can be used only at the preliminary design stage.

2. A strong exponential correlation with $R^2 > 0.93$ between the sliding probability of failure P_f and the sliding factor of safety, F_s for FORM-Taylor Series, and Monte Carlo analysis has been established.

- FORM-Taylor Series $P_{fTS} = 7.908e^{-2.421Fs}$ with $R^2 = 0.9994$
- Monte Carlo Simulation $P_{fMCS} = 19.490e^{-3.167Fs}$ with $R^2 = 0.933$

3. A very good linear correlation $P_{fTS} = 1.3227\ P_{fMCS}$ with $R^2 = 0.9542$ between the FORM-Taylor Series, $P_{fTS,}$ and Monte Carlo analysis P_{fMCS} for sliding has been obtained. FORM-Taylor P_{fTS} is 1.323 times or 32.3% more conservative than Monte Carlo analysis P_{fMCS} for sliding mode of failure.

4. Sensitivity analysis indicates that the friction angle is most dominant for the sliding mode of failure with a very high sensitivity of 91.2%, followed by the density of concrete of 8.6% sensitivity, whilst cohesion has the lowest sensitivity of only 0.2%.

5. Reliability risk analysis using Monte Carlo simulation provides a powerful tool for implementing risk reduction measures that can be utilized to assess the safety of the existing dam and provide the necessary remedial measures if the annual probability of failure surpasses 1 in 10000 per year threshold required by the guidelines.

6. There is only a marginal increase in post-tensioning design force of 4.8-6.3% (with 2- 3 additional strands required) and no changes to micro-pile size if the probability of failure needs to be decreased from the probability of failure of 10^{-4} to no likelihood of failure under each FSL, DFL, and OL event scenario. It is prudent to look into these measures as there is no implication on the construction cost and the time for completion.

7. Raked micro-piles provide a better remedial measure for sliding mode of failure than installing new post-tensioned as coring through the dam structure may jeopardize the dam's safety during the operation. Raked

micro-piles did not intrude into the dam structure's main body and interrupted the hydropower plant's operation.

Acknowledgments

The authors would like to thank the INTI International University, Malaysia for the financial support of the publication of this article.

References

[1] Barpi, F. and Valente, S. (2008), Modeling water penetration at dam-foundation joint. *Eng. Fract. Mech.* 2008, 75, 629–642. https://doi.org/10.1016/j.engfracmech.2007.02.008

[2] Brown, E.T., (2015), Rock engineering design of post-tensioned anchors for Dams: A review, *Journal of Rock Mechanics and Geotechnical Engineering* 7 (2015), 1-13. https://doi.org/10.1016/j.jrmge.2014.08.001

[3] BS8081 (2015) Code of Practice for Ground Anchors, British Standards Institution, 2015.

[4] CEB-FIP (1991), CEB-FIP Model Code 1990, *Comite Euro-International du Beton. Bulletin d'information, No. 213/214, 1991,* Lausanne.

[5] China Electric Council (2010), *The Standards Compilation of Power in China,* China Electric Council, 2010.

[6] Christian, J. T., Ladd, C. C., and Baecher, G. B. (1994), Reliability applied to slope stability analysis, *J. Geotech. Engr*., 20, Dec., 2180–2207. https://doi.org/10.1061/(ASCE)0733-9410(1994)120:12(2180).

[7] Duncan, J. M. (2000). Factors of Safety and Reliability in Geotechnical Engineering, *Journal of Geotechnical and Geo-environmental Engineering,* 127(8):700-721 https://doi: 10.1061/(ASCE)1090-0241(2001)127:8(700).

[8] Fluixá-Sanmartín, J., Altarejos-García, L., Morales-Torres, A. and Escuder-Bueno, I. (2018), Review article: Climate change impacts on dam safety, *Nat. Hazards Earth Syst. Sci.*, 18, 2471–2488, 2018. https://doi.org/10.5194/nhess-18-2471-2018.

[9] Garcia, L.A, Bueno, I.E, Lombillo, A.S. and Ortuno M.G.M, (2012) Methodology for estimating the probability of failure by sliding in concrete gravity dams in the context of risk analysis, *Structural Safety,* 36–37(2012)1–13. https://doi.org/10.1016/j.strusafe.2012.01.001.

[10] Hariri-Ardebili, M. A., Risk, Reliability, Resilience (R3) and beyond in dam engineering: A state-of-the-art review, *International Journal of Disaster Risk Reduction* 31 (2018) 806–831. https://doi.org/10.1016/j.ijdrr.2018.07.024.

[11] ICOLD (1993), International Commission on Large Dams, *Bulletin 88*: *Rock foundations for dams* ICOLD, Paris, 1993.

[12] ICOLD (2005*),* International Commission on Large Dams, *Bulletin 130: Risk assessment in dam safety management*, Paris 2005.

[13] Khan, M.D.H., Nur, S.M., El-Shafie, A. (2020), Wavelet based hybrid ANN-ARIMA models for meteorological drought forecasting, Journal of Hydrology, 590 (2020) 125380. https://doi.org/10.1016/j.jhydrol.2020.125380.

[14] Littlejohn, G.S., (1992) Rock anchorage practice in civil engineering. In: Kaiser PK, McCreath DR, eds. Rock Support in Mining and Underground Construction, Proceedings of the International Symposium on Rock Support, Sudbury. Rotterdam: A.A. Balkema, 1992: 257-68.

[15] Littlejohn, G.S., (1993) Overview of rock anchorages. In: Hudson JA, Brown ET, Fairhurst C, Hoek E, eds. Comprehensive Rock Engineering. Oxford: Pergamon Press, 1993, 4: 413-50.

[16] Melchers, R.E and Beck, A.T (2018), *Structural Reliability: analysis and prediction.* 3rd Edition, John Wiley & Sons, 2018.

[17] Muench, S. (2010). *Probabilistic User's Guide. Seattle: University of Washington.*

[18] Pei, L.; Chen, C.; He, K.; Lu, X. (2022) System Reliability of a Gravity Dam-Foundation System Using Bayesian Networks. *Reliab. Eng. Syst. Saf.* 2022, 218, 108178. https://doi.org/10.1016/j.ress.2021.108178.

[19] Pires, K.O, Beck, A.T., Bittencourt, T.N and Futai, M.M (2019) Reliability analysis of built concrete dam, *Ibracon Structures and Materials Journal,* Vol 12, Number 3 (June 2019) p 551-579. http://dx.doi.org/10.1590/S1983-41952019000300007.

[20] Phoon, K.K (2019) *Reliability-Based Design in Geotechnical Engineering Computations and Applications*, Published December 12, 2019 by CRC Press, 544 Pages. https://doi.org/10.1201/9781482265811.

[21] Reclamation (2003), United States Department of the Interior, Bureau of Reclamation, *"Guidelines for Achieving Public Protection in Dam Safety Decision Making,"* 15 June 2003.

[22] Scott, G.A., J.T. Kottenstette, and J.F. Steighner (2001), "Design and Analysis of Foundation Modifications for a Buttress Dam." *Proceedings, 38th U.S. Symposium on Rock Mechanics, Washington, D.C. pp. 951-957.*

[23] Sharafati, A.; Yaseen, Z.M.; Pezeshki, E. (2020) Strategic Assessment of Dam Overtopping Reliability Using a Stochastic Process Approach. *J. Hydrol. Eng.* 2020, 25, 04020029. https://doi.org/10.1061/(ASCE)HE.1943-5584.0001938

[24] Spross, J., Johansson, F. and Larsson, S. (2014), On the use of pore pressure measurements in safety reassessments of concrete dams founded on rock. *Georisk: Assess. Manag. Risk Eng. Syst. Geohazards* 2014, 8, 117–128. https://doi.org/10.1080/17499518.2013.864172.

[25] Su, H. Z., Hu, J., Wen, Z. P. (2013) Service life predicting of dam systems with correlated failure modes, *Journal of Performance of Constructed Facilities*, vol. 27, no. 3, pp. 252–269, 2013. https://doi.org/10.1061/(ASCE)CF.1943-5509.0000308.

[26] Tang, W. H., Stark, T. D., and Angulo, M. (1999), Reliability in back analysis of slope failures, *J. Soil Mech. and Found.,* Tokyo, October 1999. https://doi.org/10.3208/sandf.39.5_73.

[27] USACE (1997). *'Engineering and design introduction to probability and reliability methods for use in geotechnical engineering.* Engr. Tech. Letter No. 1110-2-547, Department of the Army, Washington, D.C., 30 Sept. 1997.

[28] USACE (1998), *Risk-based analysis in geotechnical engineering for support of planning studies,* Engrg. Circular No. 1110-2-554, Department of the Army, Washington, D.C., 27 Feb. 1998.

[29] USACE (2000), *Planning Guidance Notebook.* United States Army Corps of Engineers, ER 1105-2-100, 2000.

[30] USACE (2014) *Safety of Dams – Policy and Procedures, US Army Corps of Engineers,* ER1110-2-1156, 31 March 2014

[31] USBR-USACE (2019) Best Practices in Dam and Levee Safety Risk Analysis, A joint publication U.S. Department of the Interior Bureau of Reclamation and U.S. Army Corps of Engineers, July 2019.

[32] Wolff, T. F. (1994), *Evaluating the Reliability of existing levees,* Rep., Res. Proj.: Reliability of existing levees, prepared for U.S. Army Engineer Waterways Experiment Station Geotechnical Laboratory, Vicksburg, Miss.,USA.

[33] Xin, C. and Chongshi, G. (2016), Risk analysis of gravity dam instability using credibility theory Monte Carlo simulation model. *SpringerPlus 5*, 778 (2016). https://doi.org/10.1186/s40064-016-2508-7.

[34] Xu, H. and Benmokrane, B. (1996), Strengthening of existing concrete dams using post-tensioned anchors: a state-of-the-art review, Canadian Journal of Civil Engineering, vol 23 ,6,1151-1171 no 6, December 1996. https://doi.org/10.1139/l96-925.

[35] Yang, Z. and Ching, J. A (2020), Novel Reliability-Based Design Method Based on Quantile-Based First-Order Second-Moment. *Appl. Math. Modell*. 2020, 88, 461–473. https://doi.org/10.1016/j.apm.2020.06.038.

[36] Zicko, K.E., Donald, A., Bruce, D.A, Kline, R.A. (2007) The Stabilization of Gilboa Dam, New York, Using High Capacity Rock Anchors: Addressing Service Performance Issues. *Proceedings of the International Conference on Ground Anchorages and Anchored Structures in Service 2007*, Institution of Civil Engineers, London, 26-27 November 2007.

Biography:

Zakaria Che Muda earned his Ph. D. degree in Built Environment from University of Malaya. He is currently a Profess or at the Department of Civil Engineering, INTI International University, Malaysia. He has published over 100 papers in international journals. His research interests are focused on approximate analytical methods, numerical analysis, reliability-based analysis and energy efficiency.

Mohamed Hafez earned his Ph. D. degree in Geotechnical Engine ering from University of Malaya. He is currently Associate Professor at the Department of Civil Engineering, INTI International University, Malaysia. He has published over 55 papers in international journals. His research interests are focused on soft ground improvement techniques, Dam engineering numerical analysis and reliability-based analysis.

Lariyah Mohd Sidek earned his Ph. D. degree in Civil E ngineering (Urban Drainage) from Kyoto University, Japan in 2005. Currently she is a Professor and Head of Centre for Sustainable Technology and Environmental at Nasional Energy University, Malaysia. She has published about 350 papers in international conferences and journals. Her research interests include Water Resources Engineering, Dam Break Study, Risk Informed Decision Making on Dam Safety.

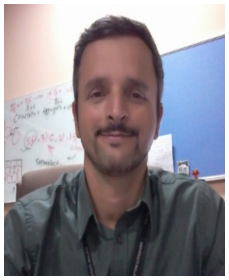

Payam Shafigh earned his Ph. D. in Structural Engineering from University of Malaya in 2013. He is currently a Professor at College of Architecture and Energy Engineering, Wenzhou University of Technology, China. He has published over 100 papers in international journals. His research interests include Lightweight Concrete Structures, Concrete Thermal Properties, Roller Compacted Concrete, Rehabilitation of Concrete Structures.

Salmia Beddu earned his Ph. D. degree in Civil Engineering from University of Petronas, Malaysia in 2012. Currently she is a Senior Lecturer at Nasional Energy University, Malaysia. She has published about 166 papers in conference proceedings and journals. Her research interests include Green Concrete, Composite Materials and Environmental Engineering.

As'ad Zakaria is currently a Ph. D student at the Institute of Energy Systems, School of Engineering, University of Edinburgh, Edinburgh, UK. He has published more than 10 papers in international journals. His research interest is in electric vehicle, power system analysis and renewable energy system.

Zaher Almakahal is currently a Graduate Research Assistance and Master student at the Department of Civil Engineering, INTI International University, Malaysia. He has published more than 10 papers in international journals and conferences. His research interests are focused on approximate analytical methods, numerical analysis, reliability-based analysis.

APPENDIX 1

TITLE: FULL SUPPLY LEVEL (S1) - EXTREME UPLIFT (D2) EXISTING DAM -NO MITIGATION MEASURE

The Area of Concrete in m^2 is 749

The Area of Water in m^2 is 219.1500

The Weight of water in kN is 2.1499e+03

The Submerged Density of silt in kg/m^3 is 9

The Area of silt in m^2 is 39.4300

The Weight of Silt in kN is 354.8700

The Total Uplift force in kN is 7.3820e+03

The Total Horizontal Hydraulic force upstream

in kN is 7.0828e+03

The Total Horizontal silt force upstream

in kN is 324.5200

The Total Horizontal Tail Hydraulic force

Downstream in KN is 122.6300

The Area of Contact m2 is 35

Total Number of Monte Carlo Sample is 10000000

Total Number of Failures out of Total Samples are 888400

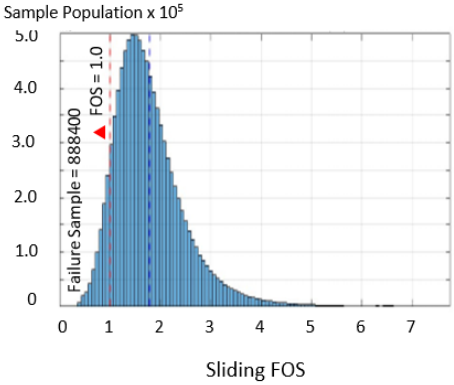

TITLE: OPTION 1 POST-TENSIONED (45º) AT FULL SUPPLY LEVEL (S1) - EXTREME UPLIFT (D2)

The Area of Concrete in m^2 is 749

The Area of Water in m^2 is 219.1500

The Weight of water in kN is 2.1499e+03

The Submerged Density of silt in kg/m^3 is 9

The Area of silt in m^2 is 39.4300

The Weight of Silt in kN is 354.8700

The Total Uplift force in kN is 7.3820e+03

The Total Horizontal Hydraulic force

In kN is 7.0828e+03

The Total Horizontal silt force upstream

In kN is 324.5200

The Total Horizontal Tail Hydraulic

Downstream in kN is 122.6300

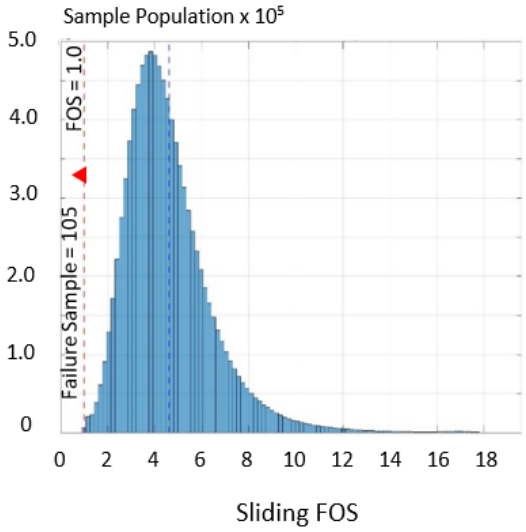

Option 1 Post-tensioned at 45º

The Vertical Post-tension force downstream

In kN/m is 3355

The Horizontal Post-tension force downstream

In kN/m run is 3355

The Area of Contact m2 is 35

Total Number of Monte Carlo Sample is 10000000

Total Number of Failures out of Total Samples are 105

Probability of Failure is 1.0500E-05

TITLE: OPTION 2 HORIZONTAL LOAD ON PILE: AT S1 FULL SUPPLY LEVEL (D2 EXTREME UPLIFT)

The Area of Concrete in m^2 is 749

The Area of Water in m^2 is 219.1500

The Weight of water in kN is 2.1499e+03

The Submerged Density of silt in kg/m^3 is 9

The Area of silt in m^2 is 39.4300

The Weight of Silt in kN is 354.8700

The Total Uplift force in kN is 7.3820e+03

The Total Horizontal Hydraulic force upstream

In kN is 7.0828e+03

The Total Horizontal silt force upstream in kN is

324.5200

The Total Horizontal Tail Hydraulic force

Downstream in kN is 122.6300

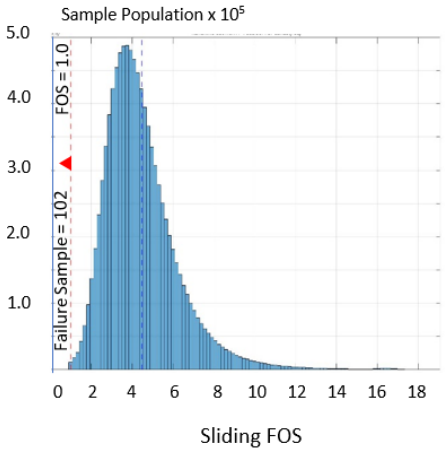

Option 2 Horizontal Load on Micro-piles

Horizontal Pile Load in kN/m is 4201

The Area of Contact m2 is 35

Total Number of Monte Carlo Sample is 10000000

Total Number of Failures out of Total Samples are 102

Probability of Failure is 1.0200E-05